DETC2008-49410

A REVIEW OF RECENT PHASE TRANSITION SIMULATION METHODS: TRANSITION PATH SEARCH

Vernet Lasrado
Department of Industrial Engineering
& Management Systems
University of Central Florida
Orlando, FL 32816, U.S.A.

Devendra Alhat
Department of Metallurgical
Engineering & Materials Science
Indian Institute of Technology-
Bombay,   Mumbai 400076, India

Yan Wang[*]
Department of Industrial Engineering
& Management Systems
University of Central Florida
Orlando, FL 32816, U.S.A.
Email: wangyan@mail.ucf.edu

ABSTRACT

In this paper, we give a review of recent transition path search methods for nanoscale phase transition simulation A potential energy surface (PES) characterizes detailed information about phase transitions where the transition path is related to a minimum energy path on the PES. The minimum energy path connects reactant to product via saddle point(s) on the PES. Once the minimum energy path is generated, the activation energy required for transitions can be determined. Using transition state theory, one can estimate the rate constant of the transition. The rate constant is critical to accurately simulate the transition process with sampling algorithms such as kinetic Monte Carlo.

1   NOMENCLATURE

PES	Potential energy surface
MEP	Minimum energy path
$\mathbf{Q}_O$	Vector of the molecular conformation of the reactant in reaction coordinates on the PES with respect to its time (t) in the reaction i.e. t=0
$\mathbf{Q}_F$	Vector of the molecular conformation of the product in reaction coordinates on the PES with respect to its time (t) in the reaction i.e. t=F
$\mathbf{Q}_X$	Vector of the molecular conformation of a point in reaction coordinates on the PES with respect to its time (t) in the reaction i.e. t=X
V	Potential Energy
∇	Gradient

2   INTRODUCTION

In this paper, we give a review of recent transition path

search methods for nanoscale phase transition simulation. It is not in the scope of this review to compare the methods against each other. Rather, we aim to provide the reader with the essence of each method reviewed.

A phase transition is a geometric and topological transformation process of materials from one phase to another, each of which has a unique and homogeneous physical property. The most important step involved in modeling phase transition is the knowledge of the activation energy barrier and rate constant involved in the transition.

In 1931, Erying and Polanyi proposed the transition state theory (TST) as a means to calculate the activation energy and rate constants [1,2] for characterizing reactions. An activation energy barrier always exists between phases. This activation energy characterizes the transition state. The methods reviewed are built on the theory prescribed by TST or some variants of TST (Variational Transition State Theory [3] and Reaction Path Hamiltonian [4])

In an effort to simulate a reaction or transition, a potential energy surface (PES) that characterizes the process is first generated. Then, a minimum energy path (MEP) is computed which represents the transition pathway in the reaction coordinate space. Finally, the activation energy and rate constant that define the speed of the process (the rate of the reaction) can be calculated using TST and information about the saddle point(s).

---

[*] All correspondence to this author
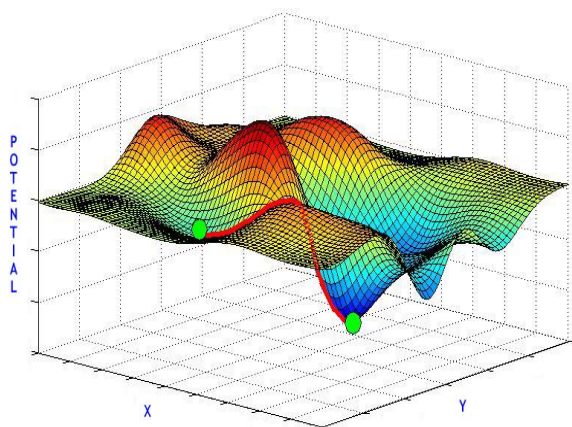
Figure 1. An illustration of the MEP on the PES where two degrees of freedom (x and y) vary while the other dimensions are fixed.
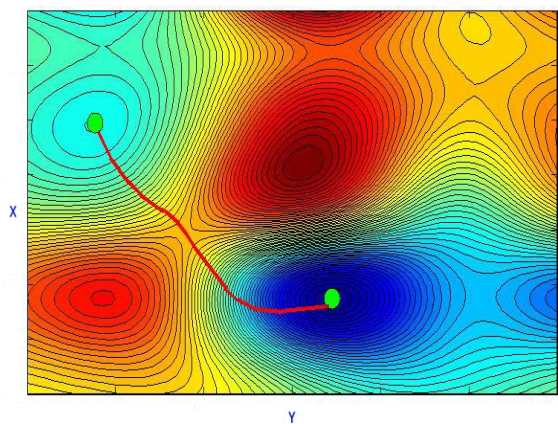
Figure 2. An illustration of the MEP on a contour plot the PES where two degrees of freedom (x and y) vary while the other dimensions are fixed.

A major challenge in searching MEP is the generation of the PES accurately. Reference [5] provides a detailed review of available methods to generate the PES characterizing information regarding the interatomic and intermolecular interactions that characterize the reaction. Also listed are some examples of methods one could use to generate the PES [6,7,8,9,10,11]. Libraries and repositories of PES are also available and ready for use [12]. Further discussion of these methods is beyond the scope of this review.

The MEP can be interpreted as the steepest descent path on the PES from saddle point(s) connecting the reactant and the product [13]. An important property of the MEP is that the direction of the gradient of the potential energy at any point on the MEP is the tangent direction along the MEP at that point. At the same time, for any degree of freedom perpendicular to the MEP at that point, the gradient of the potential energy is zero i.e. stationary [13,14].

Mathematically speaking, on the PES, the transition state is the first-order saddle point[1] (hence forth referred to as 'saddle point') located between the local minima, i.e. the reactant and product along the MEP. Once the MEP is generated, the saddle point(s) can be extrapolated. Then using transition state theory one can estimate the activation energy and the transition rate constant. The kinetic Monte Carlo (KMC) simulation [15,16] can be applied to simulate the rare events of transitions in a longer time scale than traditional molecular dynamics simulations.

Figure 1 illustrates the MEP on a hypothetical PES. The two green circles represent the reactant (higher circle relative to the "POTENTIAL" axis) and the product. The red line represents the MEP on the PES. Figure 2 illustrates the contour plot for the same PES, the area within the black circle is the saddle point region. One needs to traverse the PES from the reactant to the product to translate the MEP and thereby find the activation energy and the rate of the reaction or transition.

Since 1970, there have been many methods developed to search and identify the transition state [17,18,19], while [20,21] are older influential methods circa 1980. With the recent advancement of computational capability and computational chemistry, the systematic generation of PES with fine resolution becomes possible. Various numerical methods to search transition paths and saddle points have been developed in the recent decade. Some review papers [22,23,24] were published. However, there have been new methods and improvements that have yet to be documented. The focus of this paper is to review these latest advancements.

We categorize the computational modeling methods into two types: transition path search methods and saddle point search methods. Transition path search methods generate the MEP on the PES while saddle point search methods aim at finding the saddle points on the PES. Reference [25] provides a review saddle point search methods for phase transition simulations. In this paper, we will discuss the various methods to generate the MEP on a PES.

In the remainder of this paper, we characterize the transition path search methods into *Chain of States* methods and *Other Methods*. We can define *Chain of States* methods as methods in which the transition pathway is divided into a number of intermediate states that are relaxed and linked to finally reveal the MEP, while *Other* methods in the scope of this paper are methods that cannot be characterized as *Chain of States* methods, however, these methods generate the MEP in a different manner.

For the *Chain of States Methods*, we review the Nudge Elastic Band (NEB) method [14] along with its improvements [26,27,28,29] and the String method [30,31] along with its improvements [32,33,34]. For the *Other Methods*, we review the Conjugate Peak Refinement (CPR) method [35], the Accelerated Langevin Dynamics (ALD) method [36], and the

---

[1] A first-order saddle point has only one negative Eigen value in the Hessian matrix to the PES.

Hamilton-Jacobi method [37].

3 CHAIN OF STATES METHODS

In chain of states methods, the transition pathway is divided into a number of intermediate states. One could imagine the intermediate states as snapshots of the configuration of the atoms as they transform from initial to final state along the transition pathway. After the search converges, the intermediated states are chained to each other, usually by interpolating between the states, to obtain the transition pathway and the saddle point. They work well in transitions where there may be more than one saddle point, i.e. there may be more than one transition state. In situations where there may be multiple transition pathways, the methods will converge to the pathway closest to the initial guess for the transition pathway.

3.1 Nudge Elastic Band (NEB) Method

3.1.1 Original NEB Method [14]

The method requires that the initial and final states should be known. A number of intermediate states, usually between four and twenty, are iteratively adjusted and finally converge to the MEP keeping the initial and final state fixed.

In general, the transition path is described by a set of $P+1$ images in configuration space with reactive coordinates:

$$\mathbf{R} = \left[\mathbf{R}_0, \mathbf{R}_1, \mathbf{R}_2, ..., \mathbf{R}_P\right] \quad (1)$$

Images are connected by an imaginary elastic band. The target MEP is a group of images where the total forces acting on them reach equilibrium i.e. for any degree of freedom perpendicular to the MEP the energy is stationary. The force acting on each image is a combination of the perpendicular component of the true force due to potential energy and the parallel component of the spring force projected along the unit tangent vector to the path. The force acting on image i is given by

$$\mathbf{F}_i = -\nabla V(\mathbf{R}_i)|_\perp + \mathbf{F}_i^s|_\parallel . \quad (2)$$

The perpendicular component of the true force is give by

$$\nabla V(\mathbf{R}_i)|_\perp = \nabla V(\mathbf{R}_i) - \nabla V(\mathbf{R}_i) \cdot \hat{\boldsymbol{\tau}}_i \quad (3)$$

where V is the potential energy of the system. The unit tangent vector is given by

$$\boldsymbol{\tau}_i = \frac{\mathbf{R}_i - \mathbf{R}_{i-1}}{|\mathbf{R}_i - \mathbf{R}_{i-1}|} + \frac{\mathbf{R}_{i+1} - \mathbf{R}_i}{|\mathbf{R}_{i+1} - \mathbf{R}_i|}. \quad (4)$$

Here a normalized unit tangent vector

$$\hat{\boldsymbol{\tau}}_i = \frac{\boldsymbol{\tau}_i}{|\boldsymbol{\tau}_i|} \quad (5)$$

is used. The unit tangent vector ensures the $P+1$ images are equally spaced. The unit tangent vector uses information of both the adjacent images for image i.

The parallel component of spring force is given by

$$\mathbf{F}_i^s|_\parallel = k(|\mathbf{R}_{i+1} - \mathbf{R}_i| - |\mathbf{R}_i - \mathbf{R}_{i-1}|) \cdot \hat{\boldsymbol{\tau}}_i \hat{\boldsymbol{\tau}}_i \quad (6)$$

where k is the spring constant. At each iteration, the force acting on an image is minimized using an optimization algorithm. As a result, the images iteratively converge to the MEP. To interpret the results, one must interpolate between adjacent images to get the MEP. In the event of multiple MEP, the algorithm will converge to the MEP closest to the initial guess of the path.

The algorithm works efficiently on systems with multiple transition states, although the interpolation of the images may reveal kinks in the MEP because no perpendicular spring forces are considered. Another problem associated with NEB is that the actual saddle point may not be located by one of the images directly. Further improvements of the NEB algorithm were developed.

3.1.2 Improved Tangent Method [26]

This method is an improvement to the original NEB method [14]. The Improved Tangent method builds on the NEB method with an improved estimate of the tangent direction and a resulting change to the component of the spring force acting on the images i. This improved tangent estimate reduces the chances of getting kinks in the MEP after interpolation.

In this method, only the adjacent image with higher energy is used in computing the tangent, unless i is at a maximum or a minimum. The tangent vector from (4) is now calculated as follows

$$\boldsymbol{\tau}_i = \begin{cases} \boldsymbol{\tau}_i^+ \leftarrow V_{i+1} > V_i > V_{i-1} \\ \boldsymbol{\tau}_i^- \leftarrow V_{i+1} < V_i < V_{i-1} \end{cases} \quad (7)$$

where V_i is the potential of image i and

$$\begin{cases} \boldsymbol{\tau}_i^+ = \mathbf{R}_{i+1} - \mathbf{R}_i \\ \boldsymbol{\tau}_i^- = \mathbf{R}_i - \mathbf{R}_{i-1} \end{cases} \quad (8)$$

If the image i is at a maximum or a minimum the tangent vector is calculated based on a weighted average from the energy differences as follows

$$\boldsymbol{\tau}_i = \begin{cases} \boldsymbol{\tau}_i^+ \Delta V_i^{\max} + \boldsymbol{\tau}_i^- \Delta V_i^{\min} & \text{if } V_{i+1} > V_{i-1} \\ \boldsymbol{\tau}_i^+ \Delta V_i^{\min} + \boldsymbol{\tau}_i^- \Delta V_i^{\max} & \text{if } V_{i+1} < V_{i-1} \end{cases} \quad (9)$$

where

$$\begin{cases} \Delta V_i^{\max} = \max(|V_{i+1} - V_i|, |V_{i-1} - V_i|) \\ \Delta V_i^{\min} = \min(|V_{i+1} - V_i|, |V_{i-1} - V_i|) \end{cases} \quad (10)$$

The tangent vector has to be normalized as in (5). Finally, the spring force acting on image i is calculated as follows

$$\mathbf{F}_i^s|_\parallel = k(|\mathbf{R}_{i+1} - \mathbf{R}_i| - |\mathbf{R}_i - \mathbf{R}_{i-1}|) \cdot \hat{\boldsymbol{\tau}}_i \quad (11)$$

As a result of the above changes prescribed by (7) - (11) there is a reduction in the kinks along the MEP.

3.1.3 Climbing Image Method [27]

This method in conjunction with the Improved Tangent method [26] improves the NEB methods [14]. Once the image i_{max} with the highest energy is identified, only for i_{max} the force is calculated separately as

$$\mathbf{F}_{i_{max}} = -\nabla V(\mathbf{R}_{i_{max}}) + 2\nabla V(\mathbf{R}_{i_{max}}) \cdot \hat{\mathbf{\tau}}_{i_{max}} \hat{\mathbf{\tau}}_{i_{max}} \quad (12)$$

One may notice there is no spring component, bur rather the true force due to the potential with the component along i_{max} inverted. Therefore image i_{max} actively climbs towards the saddle point. At the same time, the spring constants are calculated differently and result in greater resolution of the images around the saddle point. The spring constants are calculated as

$$k_i' = \begin{cases} k_{max} - \Delta k \left(\dfrac{V_{max} - V_i^*}{V_{max} - V_{ref}} \right) & \text{if } V_i^* > V_{ref} \\[4mm] k_{max} - \Delta k & \text{if } V_i^* < V_{ref} \end{cases} \quad (13)$$

where $V_i^* = \max\{ V_i , V_{i-1} \}$, V_{max} is the maximum value of the energy for the entire elastic band, V_{ref} is the higher energy endpoint of the MEP , k_{max} is the maximum value to be chosen for the spring constant and Δk is the difference between k_{max} and k_{min}. The above formulation leads to a maximum spring constant if the energy is at maximum. For images that are away from this maximum energy, the corresponding spring constant approaches its minimum. This ultimately results in more images settling around the saddle point therefore achieving higher resolution.

3.1.4 Doubly Nudged Elastic Band (DNEB) Method [28]

This method is a modification to the NEB [14] method that takes into account the modifications as suggested by [26,27]. Essentially, the major change is that a manipulation of perpendicular component of the spring force $\mathbf{F}_i^{s*}$ is added to the total force (2) to give us

$$\mathbf{F}_i = -\nabla V(\mathbf{R}_i)|_{\perp} + \mathbf{F}_i^s |_{\parallel} + \mathbf{F}_i^{s*} \quad (14)$$

where

$$\mathbf{F}_i^{s*} = \mathbf{F}_i^s |_{\perp} - (\mathbf{F}_i^s |_{\perp}) \cdot \hat{\mathbf{\tau}}_i \hat{\mathbf{\tau}}_i \quad (15)$$

The band is now doubly nudged as a result of the inclusion of both the components of the spring force. The perpendicular component of the spring force for a particular image may interfere with the forces of the neighboring images. However, this is not an issue as the properties of the path are not estimated from the discrete representation of the path but rather from relaxing the paths after the convergence criterion is reached.

The authors suggest use of the limited-memory quasi-Newton (L-BFGS) optimization method [38] for the relaxation process. It approximates the Hessian matrix. For each iteration, only the *m* corrections to the Hessian are updated. The L-BFGS optimization algorithm is efficient and thus provides faster convergence of the relaxation process for each image.

In the event of multiple transition states a revised connection method is suggested. All the images where the energy of the image is greater than those of its adjacent images are separated. These distinct transition states are used to identify the minima, and they are connected by walking down the minimum energy paths. At each successive DNEB search, the new minima are stored in a database while new connections are recorded for the known minima. The DNEB method aims at building up a connected path by iteratively filling in the connections between the endpoints and the intermediate minima. This can be achieved by classifying all known minima into three sets: minima connected to a starting endpoint (S), minima connected to a final endpoint (F), and minima not connected to S or F (U). The end points separated by the shortest distance, where one endpoint belongs to either S or F, and the other belongs to U, are chosen as the endpoints for the next DNEB search.

Essentially, in the event of multiple transitions the DNEB method effectively splits the transition pathway into individual transitions. This increases the resolution for each transition state and also increases the efficiency of the relaxation process.

3.1.5 Cubic Spline Method [29]

This method is a modification to the original NEB method [14]. The authors aim at improving the efficiency of searching in the original NEB method. Two major changes are proposed, a different optimization algorithm is used to relax the images at each stage and the spring force in (2) is eliminated.

Similar to the DNEB method [28], the authors use the L-BFGS [38] method to relax the images. The next change involves eliminating the spring force from (2) and replacing it with a cubic spline.

For image *i,* the spline is generated from the 3N-dimensional representative coordinate vector. The distance between adjacent images is the arc length along the spline. The total length of the path is the sum of the distances between images. For the images to be equally spaced, the total length is divided by the number of intermediate images. This gives us a new set of coordinates for the images on the original path. A new interpolated spline then can be generated.

The authors suggest that one should reposition the images and reparameterize the spline when the spacing of the images becomes significantly distorted, i.e. if the ratio of the largest inter-image distance to the smallest such distance is greater than a certain threshold.

In the iterative searching process, one first initializes the model as in the NEB method. Then, one generates the cubic spline, gradient, tangent vector (as in improved tangent method) and the perpendicular component of the force. Then, the image with the largest force is identified and its structure is relaxed using the L-BFGS optimization algorithm. Then, a new

interpolated spline is constructed from the new structure, checking if the images need to be redistributed and the spline needs to be reparameterized. The gradient, tangent and force are recalculated. Then, one identifies the image with the largest force and the entire process is repeated.

This method greatly improves the efficiency of the NEB algorithm; most of this improvement is attributed to the use of the L-BFGS algorithm.

3.2   String Method

3.2.1   Original Method [30,31]

Similar to the NEB method, the String method is a chain of states method for locating the MEP and hence the saddle points. In the NEB, it is difficult to change the number of images, and a spring force is introduced to keep the images equidistant along the elastic band (Original NEB method). In contrast, the String method uses a smooth curve with intrinsic parameterization to represent the transition pathway. Therefore the number of discretized points along the curve can be readily increased in situations when the energy landscape is rough.

Let $\mathbf{\Psi}(\alpha, t)$ be a string connecting two minima of potential energy with α as the parameter at time t. One may either use arc length or energy weighted arc length in the parameterization. However, the energy weighted arc length provides a higher resolution at the transition state as compared to the parameterization without the energy weighted arc length. Once parameterized the string is discretized into number of points $\mathbf{\Psi}_i$ called the images on the string similar to the images $\mathbf{R}_i$ in the NEB Method.

A MEP is a smooth curve that satisfies

$$\nabla V(\mathbf{\Psi})|_{\perp} = 0 \tag{16}$$

The MEP is found by evolving the discretized φ_i according to the force given by

$$\frac{\partial \mathbf{\Psi}}{\partial t} = -\nabla V(\mathbf{\Psi})|_{\perp} \tag{17}$$

To enforce a particular parameterization constraint, a Lagrange multiplier λ is added in the tangential direction without affecting the evolvement of the curve itself, as in

$$\frac{\partial \mathbf{\Psi}}{\partial t} = -\nabla V(\mathbf{\Psi})|_{\perp} + \lambda \hat{\mathbf{\tau}} \tag{18}$$

where the unit tangent vector is given by

$$\hat{\mathbf{\tau}} = \frac{\partial \mathbf{\Psi}/\partial \alpha}{|\partial \mathbf{\Psi}/\partial \alpha|} \tag{19}$$

A reparameterization step is applied once in a while to enforce the proper parameterization of the strings.

One may use either the steepest descent method [39] or the non-linear Broyden-accelerated method [39] to converge faster. The String method can easily be generalized to infinite-dimensional dynamical systems by introducing an appropriate norm in phase space.

3.2.2   Improved String Method [32]

The original string method used the perpendicular component of the force for evolution of images as in [31]. To ensure numerical stability, the way of computing the tangent direction requires to be modified before and after the saddle points are crossed. This step lowers the accuracy of the overall method. In the Improved String method, the force projection step is eliminated. The entire force in the evolution of the images is used, given by

$$\frac{\partial \mathbf{\Psi}}{\partial t} = -\nabla V(\mathbf{\Psi}) + \lambda^* \cdot \hat{\mathbf{\tau}} \tag{20}$$

where the new Lagrange multiplier is

$$\lambda^* = \lambda + \nabla V \cdot \hat{\mathbf{\tau}} \tag{21}$$

The new representation gives more accurate results without the projection step. The new method also shows the advantage of numerical stability. It implies larger time step may be used during the string evolution. The time step limit Δt to ensure stability is not dependent of the number of images, whereas the time step limits for the original String and NEB methods are dependant on the number of images.

3.2.3   Growing String Method [33]

The Growing String method consists of a two step procedure: evolution and parameterization. The string grows from the reactant and the product end points until both ends join each other thereby trace the MEP. The number of nodes change as the number of images on the string grows.

In the evolution step, the images are moved such that the total force Eq. (22) minimized.

$$F(\mathbf{\Psi}) = \sum_{i=0}^{n} |\nabla V(\mathbf{\Psi}_i)|^2 \tag{22}$$

In the parameterization step, the images are redistributed along the string with a pre-chosen density. A new node is added to the string only if the force is smaller than a tolerance limit. This eliminates the problem associated with guessing the initial reaction pathway, thereby eliminating the dependence of speed and even the convergence of the method on initial guess. After the ends join, the iterations become identical to the original String method [30,31].

3.2.4   Quadratic String Method [34]

This method is a modification to the original String method. The method uses multi-objective optimization, which is defined as the minimization of many different functions that share the same domain [40].

The most important modification made in this method is that the integration is done locally on a quadratic PES approximation. A damped Broyden-Fletcher-Goldfarb-Shanno (BFGS) is used to update Hessian matrix [41]. The integration is performed with an adaptive step-size solver, which is restricted in length to the trust radius of the approximate Hessian. It also uses the steepest descent algorithm for

5

minimization along a direction perpendicular to the path at each point along the path.

It was claimed that the method is capable of practical super-linear convergence, in contrast to the linear convergence of other methods. One can use step size larger than that used in the original String method. The method also eliminates the need to pre-determine the step size and spring constants.

4   OTHER METHODS

4.1   Conjugate Peak Refinement Method [35]

This method iteratively finds a series of saddle points that are connected to each other and form a continuous reaction path from reactant to product. It exploits the fact that for a saddle point, the Hessian matrix (**H**) as the second derivative of the energy has exactly one negative eigenvalue. This further implies that there will be one direction along which the energy has a local maximum and k-1 directions along which the energy has a local minimum, considering k dimensions.

The method starts of guessing an initial maximum direction s_0, usually by setting the direction from reactant to product. Then maximizing the energy along s_0 and minimizing the energy along k-1 other directions iteratively yields the saddle points.

The conjugate directions are refined following

$$\mathbf{s}_1 = -\mathbf{g}_1 + \frac{\mathbf{g}_1^T \mathbf{h}}{\mathbf{s}_0^T \mathbf{h}} \mathbf{s}_0 \qquad (23)$$

and

$$\mathbf{s}_j = -\mathbf{g}_j + \frac{\mathbf{g}_1^T \mathbf{h}}{\mathbf{s}_0^T \mathbf{h}} \mathbf{s}_0 + \frac{|\mathbf{g}_j|^2}{|\mathbf{g}_{j-1}|^2} \mathbf{s}_{j-1} \text{ if } j > 1 \qquad (24)$$

where $\mathbf{g}_j$ is the gradient of the energy along $\mathbf{s}_{j-1}$.

The path generated consists of vectors (points)

$$\left[\mathbf{Q_O}, \mathbf{Q_{X1}}, \mathbf{Q_{X2}}, ..., \mathbf{Q_F}\right] \qquad (25)$$

One performs line maximization between successive points along the path (the initial path consists of just $\mathbf{Q_O}$ and $\mathbf{Q_F}$). If an energy maximum is found, line minimization is carried out along the conjugate direction to the path at the point of the energy maximum. The new point added to the path is the energy minimum along the conjugate direction from the energy maximum, in essence, a saddle point. Thus, the path is modified to include the new point. The path is refined until no further energy maximums are found along the entire path. Thus, the remaining maximum points along the path are saddle points.

The path segments are constructed by interpolating between adjacent points. The MEP can be generated after applying a minimization algorithm [39,40,41] to the path segments.

4.2   Accelerated Langevin Dynamics Method [36]

This method is a stochastic transition path sampling method by solving the Langevin equation (LE) describing the stochastic dynamics of a thermally activated system. It works in the event of multiple transition states. It is a method by which one can survey the potential energy surface, find the saddle point, and find the transition rates.

The standard dimensionless LE is given by

$$\ddot{\mathbf{Q}}_{\mathbf{X}} + \gamma\dot{\mathbf{Q}}_{\mathbf{X}} + \nabla V(\mathbf{Q}_{\mathbf{X}}) = \xi \qquad (26)$$

where γ is the dimensionless frictional coefficient and ξ is white noise with zero mean and correlations.

For a simple transition, the method starts from an initial state $(\mathbf{Q_O})$ and does not require knowledge of the final state $(\mathbf{Q_F})$. For a single transition, the pathway is divided into 2 parts: activation path and deactivation path. The activation path is the pathway from the initial state $(\mathbf{Q_O})$ to a point $(\mathbf{Q_M})$ while the deactivation path is the pathway from $(\mathbf{Q_M})$ to the final state $(\mathbf{Q_F})$. The point of separation $(\mathbf{Q_M})$ is ideally the position vector of the saddle point. Hence, ideally M is the activation time to the saddle point, which implies that, one would require a priori knowledge of the system as the efficiency of the model depends on a suitable choice of the activation time. The activation time can be best estimated if the saddle point is known or by integrating the LE and checking for a transition.

The activation path can be obtained by integrating the LE as shown in Eq.(27) from the initial conditions at $\mathbf{Q_O}$ to the conditions at $\mathbf{Q_M}$. The standard LE is modified to

$$\ddot{\mathbf{Q}}_{\mathbf{X}} - \gamma\dot{\mathbf{Q}}_{\mathbf{X}} + \nabla V(\mathbf{Q}_{\mathbf{X}}) = \xi \qquad (27)$$

The activation phase occurs with a very small probability, and direct sampling of paths by integrating Eq.(26) is not possible. The use of the negative friction coefficient (-γ) is to facilitate the generation of the activation paths by enabling the system to gain enough energy to escape from the minima at $\mathbf{Q_O}$ to the saddle point. Hence, the proposed method is poised to perform simulations at low temperatures. The deactivation path can be obtained by integrating the standard LE as in Eq.(26) from the conditions at $\mathbf{Q_M}$ to the conditions at $\mathbf{Q_F}$. For both, the activation path and the deactivation path various realizations of each can be generated by varying the white noise (ξ).

The transition path can be approximated as a weighted average of all the possible paths along the activation phase and the deactivation phase. The transition rate and the activation energy can be computed in a similar manner.

4.3   Hamilton-Jacobi Method (HJ) [37]

This method generates the MEP by solving the Hamilton-Jacobi type equation. The search is based entirely on the knowledge of the reactants $(\mathbf{Q_O})$. The information about products $(\mathbf{Q_F})$ is not required. It works on the cost principle,

that is, it assigns costs to the points on the surface. Points with higher potential energy will have a much larger cost than points with a lower potential energy. In this manner the minimum energy path has a much lower energy than other higher energy paths.

The Hamilton-Jacobi type equation may be represented as

$$\left|\nabla \tau^{(n)}\right| = \left[\frac{E - V(\mathbf{Q_X})}{E - V(\mathbf{Q_{min}})}\right]^{\frac{n}{2}} \quad (28)$$

where, $\tau^{(n)}$ is the path integral from the point $\mathbf{Q_O}$ to $\mathbf{Q_X}$ on the potential surface. It can be though of as being the level curves from $\mathbf{Q_O}$ to $\mathbf{Q_X}$, or the least arrival cost curve from $\mathbf{Q_O}$ to $\mathbf{Q_X}$ and n can be any real or integer value. In the case of finding the MEP, as n $\rightarrow$ -∞ the approximation by this method gets closer to the reaction coordinate, i.e., the MEP, thereby assigning a much higher cost to points with higher potential energy. This method often uses $\mathbf{Q_{min}} = \mathbf{Q_O}$.

The fast marching approach developed by Adalsteinsson and Sethian [42] is used to solve the Hamilton-Jacobi type equation of Eq.(28) to compute $\tau^{(n)}$ for new grid points. Essentially, the HJ method builds a set of points by marching outwards from $\mathbf{Q_O}$, keeping $\tau^{(n)}(\mathbf{Q_O}) = 0$, while sequentially adding other grid points that are the lowest-cost grid points, i.e. point with the lowest $\tau^{(n)}$. In this manner the $\tau^{(n)}$ curve is generated. Then one needs to follow the steepest descent path from $\mathbf{Q_F}$ to $\mathbf{Q_O}$. Thus, the near-MEP can be constructed by following the negative gradient direction of

$$C(s) = -\frac{\nabla \tau^{(n)}}{\left|\nabla \tau^{(n)}\right|} \quad (29)$$

The algorithm is best suited to work on adiabatic potential energy surfaces.

5   CONCLUDING REMARKS

Various transition path search methods were reviewed in this paper. These methods aim at generating a MEP on a PES characterizing detailed information regarding the interatomic and intermolecular interactions that characterize the reaction detailing a rare event. We classified the methods into two types: *Chain of States Methods* and *Other Methods*.

Among the chain of states methods, the NEB method and its improvements have immense popularity among practitioners. It is a relatively simple method to implement [14]. More importantly, it can be parallelized as each image on the path can be run on a separate computer [14]. Various improvements were made to effectively reduce kinks (Improved Tangent NEB method [26]), increase the resolution of the images around the saddle point (Climbing Image NEB method [27]), improve the stability of the method during the optimization process (Doubly Nudged NEB method [28]) and improve the efficiency of the NEB method (Cubic Spline NEB method [29]).

The String Methods and its improvements are another type of chain of states method. In contrast to the NEB method, the String method uses a smooth curve with intrinsic parameterization to represent the transition pathway [30,31]. Various improvements were made to effectively improve the accuracy (Improved String method [32]), eliminate the problem associated with guessing the initial reaction pathway (Growing String method [33]) and effectively improve the efficiency of the string method (Quadratic String method [34]).

Among the other methods, the CPR method is widely used to simulate complex proteins and is effective at finding multiple transition states [35]. The ALD method which is a stochastic transition path search method that works well for low temperature simulations and thermally activated systems [36]. The HJ method is computationally efficient, robust and only requires knowledge of the reactants. It generates a very good approximation to the MEP without using the computationally expensive Hessian matrix. As in the NEB and String methods, the HJ method can be parallelized [37].

We also noticed the key to the efficiency of these methods is the optimization algorithm used while the efficacy is determined by the global scope of the algorithm, i.e. the ability to model multiple transitions. In general, most path search methods can generate the MEP for a multi-stage transition process, thereby enabling the practitioner to extract vital information such as the transition rate and the activation energy of the reaction.

REFERENCES

[1] Eyring, H., and Polanyi, M., 1931. "Ueber einfache Gasreaktionen". *Z. Phy. Chem.* **B12**, pp. 279–311.

[2] Laidler, K., and King, C., 1983. "Development of transition-state theory", *J. Phys. Chem.*, **87**, pp. 2238-2256.

[3] Truhlar, D., and Garrett, B., 1980. "Variational Transition State Theory", *Acc. Chem. Res.*, **13**, pp.440-448.

[4] Miller, H., Handy, N., and Adams, J., 1980, "Reaction Parh Hamiltonian for polyatomic molecules", *J. Chem. Phys.*, **72**, pp. 99-112.

[5] Mansoori, A., 2005. *Principles of Nanotechnology: Molecular-Based Study of Condensed Matter in Small Systems*, World Scientific, MA, USA, Ch. 2, pp 31-83.

[6] Shin, S., 1955. "On a New Method of Drawing the Potential Energy Surface", *J. Chem. Phys.*, **23**, pp. 592-593.

[7] Truhlar D., Steckler, R., and Gordon, M., 1987. "Potential Energy Surfaces for Polyatomic Reaction Dynamics", *Chem. Rev.*, **87**, pp. 217-236.

[8] Brenner, D., and Bean, C., 1990. "Empirical potential for hydrocarbons for use in simulating the chemical vapor

deposition of diamond films". *Phys. Rev. B*, **42**, pp. 9458-9471.

[9] Thompson, K., Jordan, M., and Collins, M., 1998. "Molecular potential energy surfaces by interpolation in Cartesian coordinates", *J. Chem. Phys.*, **108**, pp. 564-578.

[10] Hollebeek, T., Ho, T., and Rabitz, T., 1999. "Constructing multidimensional molecular potential energy surfaces from ab initio data", *Ann. Rev. of Phys. Chem.*, **50**, pp. 537-570.

[11] Burke, M., and Yaliraki, S., 2006. "Exploring Model Energy and Geometry Surfaces using Sum of Squares Decomposition", *J. Chem. Theory Comput.*, **2**, pp. 575-587.

[12] Duchovic, R., Volobuev, Y., Lynch, G., Truhlar, D., Allison, T., Wagner, A., Garrett, B., and Corchado, J., 2002. "POTLIB: A potential energy surface library for chemical systems", *Comp. Phys. Comm.*, **144**, pp. 169-187.

[13] Quapp, W., and Heidrich, D., 1984. "Analysis of the concept of minimum energy path on the potential energy surface of chemically reacting systems", *Theo. Chem. Acc.*, **66**, pp. 245-260.

[14] Jonsson, H., Mills, G., and Jacobsen, K., 1998. *Classical and Quantum Dynamics in Condensed Phase Simulations*. World Scientific, Hackensack, NJ, Chap. 16, pp. 385-404. See also URL http://www.hi.is/~hj/paperNEBleri.pdf

[15] Gillespie, D., 1977. "Exact stochastic simulation of coupled chemical reactions", *J. Phys. Chem.*, **81,** pp. 2340-2361.

[16] Henkelman G., Jónsson H., 2001. "Long time scale kinetic Monte Carlo simulations without lattice approximation and predefined event table", *J. Chem. Phys.*, **115**, pp. 9657-9666.

[17] Fukui, K., Kiato S., and Fujimoto, H., 1975. "Constituent analysis of the potential gradient along a reaction coordinate. Method and an application to methane + tritium reaction.", *J. Am. Chem. Soc.*, **97**, pp. 1-7.

[18] Müller, K., 1980. "Reaction paths on Multidimensional Energy Hypersurfaces", *Angew. Chem. Int. Ed. Engl.* **19**, pp. 1-13.

[19] Cerjan, C., and Miller, W., 1981. "On finding Transition States", *J. Chem. Phys.*, **75**, pp. 2800-2806.

[20] Laider, K., and King, M., "The Development of Transition State Theory". *J. Phys. Chem.*, **87**, pp. 2657-2664.

[21] Trulhar, D., Hase, W., and Hynes, J., 1983. "Current Status of Transition-state Theory", *J. Phys. Chem.*, **87**, pp. 2664-2682.

[22] Henkelman, G., Johannesson, G., and Jonsson, H., 2002. *Theoretical Methods in Condensed Phase Chemistry*, Vol. 5 of *Progress in Theoretical Chemistry and Physics*, Springer, Netherlands, Ch. 10, pp 269-302. Available at http://www.springerlink.com/content/g08075gph6825331/

[23] Schlegel, H., 2003. "Exploring potential energy surfaces for chemical reactions: An overview of some practical methods", *J. Comp. Chem.*, **24**, 1514-1527.

[24] Olsen, R., Kroes, G., Henkelman, G., Arnaldson, A., and Jonsson, H., 2004 . "Comparison of Methods for Finding Saddle Points without Knowledge of the final states", *J. Chem. Phys.*, **121**, 9776-9792.

[25] Alhat, D., Lasrado, V., Wang, Y., 2008. "A Review of Phase Transition Simulation: Saddle Point Search Methods", *Proc. IDETC08*, paper No. DETC2008-49411.

[26] Henkelman, G., and Jonsson, H., 2000. "Improved tangent estimate in the nudged elastic band method for finding minimum energy paths and saddle points", *J. Chem. Phys.*, **113**, pp. 9978-9985.

[27] Henkelman, G., Uberuaga, B., and Jonsson, H., 2000. "A climbing image nudged elastic band method for finding saddle points and minimum energy paths", *J. Chem. Phys.*, **113**, pp. 9901-9904.

[28] Trygubenko, S., and Wales, D., 2004. "A doubly nudged elastic band method for finding transition states", *J. Chem. Phys.*, **120**, 2082-2094.

[29] Galvan, I., and Field, M., 2008. "Improving the Efficiency of the NEB Reaction Path Finding Algorithm", *J. Comp. Chem.*, **29**, pp. 139-143.

[30] E, W., Ren, W., and Vanden-Eijnden, E., 2002. "String method for the study of rare events", *Phys. Rev. B*, **66**, pp. 052301(1)-052301(4).

[31] Ren, W., 2003. "Higher order string method for finding minimum energy path", *Comm. Math. Sci.*, **1**, pp. 377-384.

[32] E, W., Ren, W., and Vanden-Eijnden, E., 2007. "A Simplified and improved string method for computing the minimum energy paths in barrier-crossing events", *J. Chem. Phys.*, **126**, pp. 164103(1) -164103(8).

[33] Peters, B**.,** Heyden, A., Bell, A., and Chakraborty, A., 2004. "A growing string method for determining transition states: Comparison to the nudged elastic band and string methods", *J. Chem. Phys.*, **120**, 7877-7886.

[34] Burger, S., and Yang, W., 2006. "Quadratic string method for determining the minimum-energy path based on multiobjective optimization", *J. Chem. Phys.*, **124**, pp. 054109(1)- 054109(12) .

[35] Fischer, S., and Karplus, M., 1992. "Conjugate Peak Refinement: an algorithm for finding reaction paths and accurate transition states with many degrees of freedom", *Chem. Phys. Lett.*, **194**, 252-261.

[36] Chen, L., Ying, C., and Ala-Nissila, T., 2002. "Finding transition paths and rate coefficients through accelerated Langevin dynamics", *Phys. Rev. E*, **65**, pp. 042101(1)-042101(4).

[37] Dey, B., and Ayers, P., 2006. "A Hamilton–Jacobi type equation for computing minimum potential energy paths", *Mol. Phys.*, **104**, pp. 541–558.

[38] Liu, D., and Nocedal, J., 1989. "*On the limited memory BFGS method for large scale optimization*", J. Math Prog., **45**, pp. 503-528.

[39] Kelly, C., 1995. *Iterative Methods for Linear and Nonlinear Equations*, Vol. 16 of *Frontiers of applied*

Mathematics, SIAM, Philadelphia, PA. Available at http://www.ec-securehost.com/SIAM/FR16.html

[40] Collette, Y., and Siarry, P., 2003. *Multiobjective Optimization*, Springer, New York, NY.

[41] Fletcher, R., 1987. *Practical Methods of Optimization*, Wiley, New York, NY.

[42] Adalsteinsson, D., and Sethian, J., 1995. "A Fast Level Set Method for Propagating Interfaces," *J. Comp. Phys.*, **118**, pp. 269-277.